of CH_3 vs CH_2D groups.[26] For **1** and **1-d_6**, the difference in zero-point energies should lead to a different barrier to ring equilibration if the bond-breaking mechanism shown in the top of Figure 5 is correct, but the barrier would be the same for the rotational motion shown in the bottom of Figure 5.

Figure 7 shows the ^{13}C NMR spectra of the most deshielded resonance of **1** and **1-d_6** in the temperature range of their coalescence. In the limiting low-temperature spectrum (-83 °C), the separation of the resonances for both complexes is the same (11.3 Hz) and both have the same half-height width. Thus, no isotope effects or C-D coupling is observed in these resonances for **1-d_6**. At -59 °C, the resonances are collapsing such that the separation is 5.1 Hz for **1** and 4.4 Hz for **1-d_6**. At -56 °C, **1-d_6** is at its coalescence temperature whereas a separation of 4.3 Hz is still observed for **1**. Coalescence is reached for **1** at -53 °C. The calculated energy difference for the two molecules is only 0.2 kcal/mol, but the spectra clearly indicate a difference. While not large, this difference strongly indicates that the process that equilibrates the pyrazolyl rings involves bond breaking of the B-H···Y interaction. Thus, both of the fluxional processes observed for **1** are believed to be caused by the molecular motion shown in the top of Figure 5.

Conclusions

The complexes $[H(\mu\text{-}H)B(pz)_2]_3Y$ (**1**) and $[H(\mu\text{-}H)B(3,5\text{-}Me_2pz)_2]_3Y$ (**2**) are readily prepared from YCl_3 and the ligand salt. The solid-state structure of **1** has been determined crystallographically. It consists of a trigonal-prismatic arrangement of the nitrogen donor atoms with each of the three rectangular faces capped by a bridging, three-center B-H···Y interaction. The bridging interaction is confirmed in both the solid and solution phases for **1** and **2** by the observation of low B-H stretching bands in the IR and in solution by the nonequivalence of the BH_2 resonances in low-temperature NMR spectra. The pyrazolyl rings of both complexes also show as a 1/1 nonequivalent set in low-temperature ^{13}C NMR spectra. The molecules show dynamic rearrangements in solution with both the BH_2 proton and pyrazolyl carbon signals collapsing to a single set of resonances above 0 °C. This observation for the BH_2 group was confirmed from ^2H NMR data on $[D(\mu\text{-}D)B(pz)_2]_3Y$ (**1-d_6**). As the pyrazolyl rings are equivalent in the solid-state structure, we propose in solution that the triangular faces of the trigonal prism are rotated toward an octahedral type arrangement. The dynamic processes that equilibrate the BH_2 and pyrazolyl rings have very similar barriers and are believed to arise from a single molecular rearrangement. The mechanism proposed involves breaking the three-center interactions, flipping the boat-shaped YN_4B rings, and re-forming the three-center interactions on the other adjacent faces. This mechanism is supported by the measurement of a slightly different barrier to equilibration of the pyrazolyl rings in **1** vs that in **1-d_6**.

Acknowledgment. We wish to thank Dr. Paul Ellis for running the solid-state ^{13}C NMR spectra and for useful discussions. We thank Dr. Ron Garber for assistance with the ^{89}Y NMR data and Dr. Richard D. Adams and Dr. Jack Faller (Yale University) for discussions of the variable-temperature NMR data. The NSF (Grant CHE-8411172) and NIH (Grant RR-02425) have supplied funds to support NMR equipment, and the NIH (Grant RR-02849) has supplied funds to support mass spectrometry equipment.

Registry No. **1**·$CHCl_3$, 114094-42-7; **2**, 114094-43-8; **1-d_6**, 114094-44-9; Y, 7440-65-5.

Supplementary Material Available: Table IV (bond distances and angles for the ligands), Table V (positional parameters of H atoms), and a table listing anisotropic thermal parameters (6 pages); a table of structure factor amplitudes (14 pages). Ordering information is given on any current masthead page.

(26) (a) Calvert, R. B.; Shapley, J. R. *J. Am. Chem. Soc.* **1978**, *100*, 7726. (b) Casey, C. P.; Fagan, P. J.; Miles, W. H. *J. Am. Chem. Soc.* **1982**, *104*, 1134.

Contribution from the Department of Chemistry, State University of New York at Albany, Albany, New York 12222

Synthesis and Structural Characterization of a Tetramolybdate, $[Mo_4O_{12}(C_8H_6N_4)]^{2-}$, Containing a Bridging Phthalazine-1-hydrazido(2-) Ligand. Comparison to the Structure of $[Mo_4O_{10}(OMe)_2(NNMePh)_2]^{2-}$, a Tetramolybdate Species Exhibiting Ligation to a Terminal Monodentate Hydrazido(2-) Group

Shahid N. Shaikh and Jon Zubieta*

Received October 23, 1987

The reaction of $(n\text{-}Bu_4N)_2[Mo_2O_7]$ with 1-methyl-1-phenylhydrazine in CH_2Cl_2-methanol yields the tetranuclear poly oxomolybdate $(n\text{-}Bu_4N)_2[Mo_4O_{10}(OCH_3)_2(NNMePh)_2]$ (I). Complex I displays the methoxy-bridged binuclear core $[MoO(NNMePh)(\mu\text{-}OCH_3)_2MoO(NNMePh)]^{2+}$, bridged by two double-bridging bidentate $[MoO_4]^{2-}$ units. Complex I is structurally related to the class of tetranuclear poly oxomolybdates coordinated to small organic molecules, $[Mo_4O_{6-10}L_1L_2]^{n-}$. The reaction of $(n\text{-}Bu_4N)_2[Mo_2O_7]$ with the potentially chelating and bridging hydrazino ligand hydrazinophthalazine, $H_2NNH(C_8H_5N_2)$ (H_2NNH-pht), yields the analogous tetranuclear species $(n\text{-}Bu_4N)_2[Mo_4O_{12}(HNN\text{-}pht)]$ (II). Although structurally related to I, II reveals a number of distinctive features. The binuclear core $[Mo_2O_4(HNN\text{-}pht)]^{2+}$ displays a bridging oxo group and a bidentate bridging phthalazine moiety, in contrast to the two bridging methoxy groups of I. The Mo centers of this core are nonequivalent, one exhibiting $[MoO_4N_2]$ coordination and the other $[MoO_5N]$. The bridging $[MoO_4]^{2-}$ moieties display unexceptional geometry. The ^{17}O NMR spectra of I, II, and the related 1,4-dihydrazinophthalazine derivative $[Mo_4O_{11}(C_8H_6N_6)]^{2-}$ are consistent with the solid-state structures, exhibiting resonances in the regions assigned to doubly bridging Mo_2O groups (350-450 ppm) and to terminal MoO groups (750-950 ppm). Crystal data follow. For I: monoclinic space group $P2_1/c$, with a = 9.770 (2) Å, b = 18.633 (3) Å, c = 16.706 (3) Å, β = 90.74 (1)°, V = 3041.0 (12) Å, Z = 2, and D_{calcd} = 1.45 g cm^{-3}; structure solution based on 1571 reflections converged at R = 0.0647. For II: triclinic space group $P\bar{1}$, with a = 16.528 (2) Å, b = 17.631 (3) Å, c = 19.539 (4) Å, α = 88.90 (1)°, β = 87.00 (1)°, γ = 88.10 (1)°, V = 5682.2 (24) Å^3, Z = 4, and D_{calcd} = 1.43 g cm^{-3}; structure solution based on 5429 reflections converged at 0.0689.

The coordination compounds of isopoly oxomolybdates continue to attract considerable attention as models for the interactions of small organic molecules with catalytic oxide surfaces.[1,2] The coordination chemistry of the isopoly oxomolybdate anions with

0020-1669/88/1327-1896$01.50/0

oxygen donor ligands has been developed to include a variety of derivatized octanuclear and tetranuclear clusters[3-5] exhibiting pseudooctahedral molybdenum centers, $[MoO_6]$. Although the ligation of nitrogen donors had been limited to the pyridine complex $[(C_5H_5N)_2Mo_8O_{26}]^{4-}$, which again displayed octahedral metal cores $[MoO_5N]$ or $[MoO_6]$[2], we have recently extended the nitrogen donor chemistry to include of variety of diazenido- and hydrazido-derivatized clusters of the general class $[Mo_4O_{12-n}(NN-)_n]^{2-}$ (n = 2 or 4).[7-12] An unusual feature of these tetranuclear clusters is the presence of tetrahedral molybdenum centers $[MoO_4]$ in addition to octahedral sites of the type $[MoO_4N_2]$ and $[MoO_5N]$. The tetranuclear core appears to be characteristic of derivatized isopoly molybdates in orgnic solvents, such that the core is sufficiently robust to accommodate substitution reactions at the surface oxo groups to yield complexes of the general class $[Mo_4O_6(OR)_2(XC_6H_4Y)_2(NNR)_4]^{2-}$, where the pseudo-square-pyramidal Mo(VI) core $[MoO_4N]$ has been identified.[12]

In the course of these continuing investigations of the interactions of poly oxomolybdates with substituted hydrazines, we have examined the reaction chemistry of 1-hydrazinophthalazine, $H_2NHN(C_8H_5N_2)$, a hydrazino-type ligand capable of chelating interactions utilizing the α-nitrogen of the hydrazine residue and the nitrogen donors of the phthalazine substituent. By exploiting the chelating and bridging abilities of the hydrazinophthalazine ligand we sought to expand the synthetic and structural chemistry of the tetramolybdate core[8-12] to a novel area of organodinitrogen ligation. While this work was in progress, the structure of a related tetramolybdate $[Mo_4O_{11}(dhphH_2)]^{2-}$ (anion of III), containing the quadruply deprotonated form of the binucleating ligand 1,4-dihydrazinophthalazine, was reported.[13] In this paper, the structure of the title cluster $[Mo_4O_{12}(HNN\text{-}pht)]^{2-}$ (anion of II) is compared to that of III, and the ^{17}O spectra of these species are discussed with reference to that of the previously reported hydrazido(2-) cluster $[Mo_4O_{10}(OMe)_2(NNMePh)_2]^{2-}$.[10]

Experimental Section

Solvents were purchased from Aldrich. Methylphenylhydrazine was purchased from Eastman Chemicals, and hydralazine hydrochloride from Alfa. The parent isopolymolybdate, $(n\text{-}Bu_4N)_2[Mo_2O_7]$, was prepared by the literature method.[14] All manipulations were carried out under purified N_2 by using standard Schlenk techniques. Pentane was dried by the published procedure.[15] Acetonitrile was dried over CaH_2. Anhydrous ether was passed through activated alumina prior to use. Elemental analyses were performed by Desert Analytics, Tuscon, AZ. The instrumentation used to obtain electronic and infrared spectra and X-ray diffraction data have been described previously.[16] Electrochemical investigations were performed on a BAS 100 electroanalytical system. Solutions used in cyclic voltammetric studies were 3×10^{-3} M in complex and 0.1 M in $(n\text{-}Bu_4N)PF_6$ in acetonitrile.

Synthesis of $[Mo_4O_{10}(\mu\text{-}OCH_3)_2(NNCH_3C_6H_5)_2][n\text{-}C_4H_9)_4N]_2$ (I). Method A. White crystalline $[Mo_2O_7][(n\text{-}C_4H_9)_4N]_2$ (9.51 g, 12.06 mmol) was placed in a 500-mL Schlenk flask, which was fitted with an addition funnel and evacuated/purged with N_2 three times. 1-Methyl-1-phenylhydrazine (8.8372 g, 72.33 mmol) was dissolved in 100 mL of CH_2Cl_2/CH_3OH (1:1, v/v) and placed in the addition funnel. This mixture was purged with N_2 for 10 min and then added to the $[Mo_2O_7](n\text{-}Bu_4N)_2$ with stirring. While the flask contents were stirred at room temperature for 24 h, the color gradually changed from light yellow to a dark orange clear solution. A 200-mL pentane–diethyl ether (2:1 V/V) mixture was gently layered over this solution. After the mixture was allowed to sit for 2 weeks at room temperature, orange crystals formed. These were separated, washed with ether, and vacuum dried; yield 5.25 g (65.3%). Anal. Calcd for $C_{48}H_{94}Mo_4N_6O_{12}$: C, 43.31; H, 7.12; N, 6.31. Found: C, 43.37; H, 7.35, N, 6.26. IR (KBr disk, cm^{-1}): 1594 (s), 1480 (s), 1370 (s), 1132 (w), 923 (s), 900 (vs), 770 (vs, br), 700 (w), 530 (w). UV/vis in CH_2Cl_2 [λ_{max}, nm (ϵ, M^{-1} cm^{-1})]: 337 (2.4×10^4), 273 (3.7×10^4).

Method B. The preparation was carried out in a manner analogous to that described above. A 100-mL Schlenk flask was charged with $[(n\text{-}C_4H_9)_4N]_4[Mo_8O_{26}]$ (1.0 g, 4.64×10^{-4} mol) and 1-methyl-1-phenylhydrazine (0.3404 g, 2.78 mmol) in 40 mL of CH_3OH was added. The flask contents were stirred at room temperture for 12 h, to obtain a clear dark orange solution, which was layered with 80 mL of pentane/ether (1:1, v/v). Upon when this mixture was allowed to stand at room temperature for 2 weeks, orange crystals formed. Yield: 0.62 g (50.2%). Anal. Calcd for $C_{48}H_{94}Mo_4N_6O_{12}$: C, 43.31; H, 7.12, N, 6.31. Found: C, 43.27; H, 7.25; N, 6.36 IR (KBr pellet, cm^{-1}) 1593 (s), 1486 (s), 1265 (m), 1160 (m), 1023 (s), 917 (sh), 895 (vs), 7985 (vs), 765 (vs), 680 (s). UV/vis in CH_2Cl_2 [λ_{max} nm (ϵ, M^{-1} cm^{-1})]: 340 (2.4×10^4), 278 (3.7×10^4).

Synthesis of $[Mo_4O_{12}(C_8H_6N_4)][(n\text{-}C_4H_9)_4N]_2 \cdot 0.5CH_3CN$ (II). To a stirred solution of $[Mo_2O_7][(n\text{-}C_4H_9)_4N)]_2$(5.0g, 6.34 mmol) in dry CH_3CN (100 mL) at 25 °C was added solid hydralazine hydrochloride (2.497 g, 12.68 mmol). The color of the reaction mixture immediately changed to dark brown. After 15 min of stirring, the solution was filtered to remove undissolved brown precipitate. The precipitate was washed with CH_3CN (150 mL) until the washings were free of brown color. The above filtrate along with the washings was then layered slowly with anhydrous diethyl ether (250 mL). Cooling at −10 °C for 4 weeks afforded rectangular-shaped red-brown crystals. Yield: 2.9 g (75%). Anal. Calcd for $C_{41}H_{79.5}N_{6.5}O_{12}Mo_4$: C, 39.66; H, 6.41; N, 7.34. Found: C, 39.70; H, 6.52; N, 7.41. IR (KBr disk, cm^{-1}): 3160 (m), 950 (s), 930 (s), 910 (s), 760 (s, br). UV/vis in DMF [λ_{max}, nm (ϵ, M^{-1} cm^{-1})]: 482 (6.3×10^3), 272 (1.0×10^4).

Synthesis of $[Mo_4O_{11}(dhphH_2)][(n\text{-}C_4H_9)_4N]_2$ (III). To a stirred solution of $[Mo_2O_7][(n\text{-}C_4H_9)_4N]_2$ (0.5 g, 6.34×10^{-4} mol, in CH_3CN (20 mL) at 25 °C was added 1,4-dihydrazinophthalazine, ($dhphH_6$) (0.189 g, 8.36×10^{-4} mol). After 30 min, the color changed to red-brown; the solution was filtered to remove 0.1 g of insoluble precipitate and washed with CH_3CN (5 mL). Addition of 20 mL of anhydrous diethyl ether to the combined filtrate and washings was followed by storage at −10 °C. After 2 weeks, red-brown crystals along with a small amount of white precipitate formed. Yield: 0.217 g. This mixture was dissolved in Gold Label CH_3NO_2 (10 mL), filtered to remove the white precipitate, and stored at −10 °C. Over a period of 3 weeks, red-brown block-shaped crystals formed. These crystals were washed with anhydrous ether and vacuum-dried. Yield: 0.173 g (45%). Anal. Calcd for $C_{40}H_{78}Mo_4N_8O_{12}$: C, 39.03; H, 6.39; N, 9.1. Found: C, 39.60; H, 6.52; N, 9.23; IR (KBr disk, cm^{-1}): 3170 (m), 942 (ms), 932 (s), 752 (s, br). UV/vis in DMF [λ_{max} nm (ϵ, M^{-1} cm^{-1})]: 547 (2.2×10^3), 402 (1.4×10^4), 305 (1.5×10^4).

The enriched ^{17}O complex of III was prepared under N_2 by using Schlenk techniques. The crystalline complex II (0.10 g, 8.12×10^{-5} mol) was dissolved in CH_3CN (5 mL) in a 25-mL Schlenk tube and evacuated/purged with N_2 by using the freeze–thaw method. To this solution was added ^{17}O-enriched water (20 μL) via a syringe through rubber septum, and the contents were stirred for 24 h. After this solution was layered with anhydrous ether (10 mL), it was stored at −5 °C. The red-brown crystalline product was obtained in 3 weeks (60 mg, yield 60%).

^{17}O Nuclear Magnetic Resonance Spectra. A. Sample Preparation. As indicated above, samples were prepared by using 50% ^{17}O-enriched water, purchased from Cambridge Chemicals. All preparative procedures involving ^{17}O-enriched water were carried out in a closed system in order to prevent isotopic dilution by atmospheric water. The ^{17}O-enriched sample of α-$[Mo_8O_{26}][Bu_4N]_4$ and $(n\text{-}Bu_4N)_2[Mo_2O_7]$ were prepared by the literature method of Holm et al.[17] The ^{17}O-enriched samples of the hydralazine- and hydrazido-derived complexes were pre-

(1) Pope, M. T. *Heteropoly and Isopoly Oxometalates*; Springer: New York, 1983.
(2) Day, V. W.; Klemperer, W. G. *Science (Washington, D.C.)* **1985**, *228*, 533.
(3) Adams, R. D.; Klemperer, W. G.; Liu, R.-S. *J. Chem. Soc., Chem. Commun.* **1979**, 256.
(4) McCarron, E. M., III; Harlow, R. L. *J. Am. Chem. Soc.* **1983**, *105*, 6179.
(5) Day, V. W.; Frederick, M. F.; Klemperer, W. G.; Liu, R.-S. *J. Am. Chem. Soc.* **1979**, *101*, 491. Day, V. W.; Thompson, M. R.; Day, C. S.; Klemperer, W. G.; Liu, R.-S. *J. Am. Chem. Soc.* **1980**, *102*, 5973.
(6) McCarron, E. M., III; Whitney, J. F.; Chase, D. B. *Inorg. Chem.* **1984**, *23*, 3276.
(7) Hsieh, T.-C.; Zubieta, J. *Inorg. Chem.* **1985**, *24*, 1287.
(8) Hsieh, T.-C.; Zubieta, J. *Polyhedron* **1986**, *5*, 305.
(9) Hsieh, T.-C.; Zubieta, J. *Polyhedron* **1986**, *5*, 1655.
(10) Shaikh, S. N.; Zubieta, J. *Inorg. Chem.* **1986**, *25*, 4613.
(11) Hsieh, T.-C.; Zubieta, J. *J. Chem. Soc., Chem. Commun.* **1985**, 1749.
(12) Liu, S.; Shaikh, S. N.; Zubieta, J., unpublished results.
(13) Attanasio, D.; Fares, B.; Imperatori, P. *J. Chem. Soc., Chem. Commun.* **1987**, 1476.
(14) Filowitz, M.; Ho, R. K. C.; Klemperer, W. G.; Shum, W. *Inorg. Chem.* **1979**, *18*, 93.
(15) Gordon, A. J.; Ford, R. A. *The Chemist's Companion*; Wiley: New York, 1972.
(16) Bruce, A.; Corbin, J. L.; Dahlstrom, P. L.; Hyde, J. R.; Minelli, M.; Steifel, E. I.; Spence, J. T.; Zubieta, J. *Inorg. Chem.* **1982**, *21*, 917.
(17) Do, Y.; Simhon, E. D.; Holm, R. H. *Inorg. Chem.* **1985**, *24*, 1831.

Table I. 40.66-MHz ^{17}O NMR Data for Organonitrogen-Derivatized Poly Oxomolybdate Anion Clusters

compd	chem shift, ppm (assignment) [line width][a,b]
$[Mo_4O_{10}(NNMePh)_2]^{2-}$	425 (O1) [156], 786 (O2) [175], 936 (O3) [856]
$[Mo_4O_{12}(C_8H_6N_4)]^{2-}$	355 (O3) [84], 404 (O1, O2) [131], 463 (O1, O2) [128], 792 (O6, O7) [82], 835 (O6, O7) [106], 897 (O4) [410], 928 (O5) [190]
$[Mo_4O_{11}(C_8H_6N_6)]^{2-}$	408 (O5) [129], 445 (O1) [192], 779 (O2, O3) [81], 794 (O2, O3) [85], 937 (O4) [342]

[a] Chemical shifts are downfield from $H_2{}^{17}O$. All peak widths at half-height are given in hertz. Spectra are recorded at 297 K. No signals were observed for alkoxide oxygens. [b] Oxygen assignments refer to the labeling schemes displayed for the idealized structures in Figure 1.

pared by adjusting the conditions described above in order to minimize isotopic dilution by atmospheric oxygen. Preparations were generally carried out on a 0.50-g scale.

B. Spectral Measurements. ^{17}O NMR spectra were recorded at 297 K at 40.66 MHz by using the pulse FT NMR technique on a Varian XL-300 spectrometer interfaced with a Motorola 68000 microprocessor computer. The spectra were digitized by using 6976 or 8000 data points depending on the acquisition times and spectral bandwidths employed. The pulse width used for a 90° pulse was 25 μs. Deuteriated acetonitrile was employed as an internal lock. Spectra were obtained by using a double-precision acquisition technique in cylindrical 10-mm-o.d. sample tubes (3.0-mL sample volume) and referenced to internal $H_2{}^{17}O$. Chemical shifts are reported in parts per million with positive values in the low-field direction relative to $H_2{}^{17}O$. All chemical shifts and linewidth data were reproducible within ±2% and ±5%, respectively.

C. Spectral Parameters. The following abbreviations are used: cpd for compound, sol for solvent, [X] for molar concentration of X, NT for number of transients, AT for acquisition time in milliseconds, SW for sweep width in hertz, TO for transmitter offset in hertz, and LB for exponential line broadening in hertz. (1) cpd = $[n\text{-}Bu_4N]_2[Mo_4O_{10}(OCH_3)_2(NNMePh)_2]$ (I), sol = CD_3CN/CH_3CN(1:2), [X] = 1.44×10^{-2}, NT = 50000, AT = 50, SW = 69930, TO = 20000, and LB = 30. (2) cpd = $[n\text{-}Bu_4N]_2[Mo_4O_{12}(C_8H_5N_4)]$ (II), sol = CD_3CN/CH_3CN(1:2), [X] = 2.62×10^{-2}, NT = 50000, AT = 50, SW = 69930, TO = 20000, and LB = 30. (3) cpd = $[n\text{-}Bu_4N]_2[Mo_4O_{11}(C_8H_6N_6)]$ (III), sol = CD_3CN/CH_3CN(1:2), [X] = 1.19×10^{-2}, NT = 50000, AT = 50, SW = 69930, TO = 20000, LB = 30. Results are tabulated in Table I.

X-ray Crystallographic Studies. The details of the crystal data, data collection methods, and refinement procedures are given in Table II. Full details of the crystallographic methodologies may be found in ref 16.

One of the $(n\text{-}Bu_4N)^+$ cations of the structure of $(n\text{-}Bu_4N)_2[Mo_4O_{12}(C_8H_5N_4)]$ displayed signs of disorder: a spread in the C–C distances of ca. 0.25 Å and a number of excursions of electron density in the range of 0.75 e/Å^3 at distances compatible with carbon atom positions. Since no disorder model provided a significant improvement over the simple expedient of locating the carbon positions at the largest peaks consistent with atom positions, no attempt was made to introduce a disorder model into the final refinement cycles.

The $(n\text{-}Bu_4N)^+$ cation of the $(n\text{-}Bu_4N)_2[Mo_4O_{10}(OCH_3)_2(NNMePh)_2]$ structure exhibited problems similar to those discussed for $(n\text{-}Bu_4N)_2[Mo_4O_{11}(C_8H_6N_4)]$ and was treated in a similar fashion.

Results and Discussion

Synthesis and Spectroscopic Properties. In methanolic solution, $[Mo_2O_7]^{2-}$ has been shown to react to yield a variety of oxo–methoxy species of hexavalent molybdenum, of which $[Mo_4O_{10}(OMe)_6]^{2-}$ represents the most readily isolable product. The initial step in the synthesis of the hydrazido(2–) derivative $[Mo_4O_{10}(OMe)_2(NNMePh)_2]^{2-}$ would appear to be the formation of an equilibrium mixture of oxo–methoxy species, which subsequently react in a condensation type reaction of (Mo=O) units with $H_2NNMePh$, producing water and the $(MoNNR_2)$ unit, with concomitant cluster reaggregation to yield the tetranuclear cluster.

Reactions of $[Mo_2O_7]^{2-}$ with hydralazine and 1-hydrazinophthalazine are most conveniently carried out in acetonitrile, although products could be isolated in low yield from methanol or methylene chloride. The retention of the tetranuclear core in complexes with potentially chelating hydrazine ligands provides further support for the ubiquity of this core in nonaqueous solvents. The chemistry of the tetranuclear core has recently been expanded to include both oxygen and nitrogen donor ligands, capable of monodentate and/or terminal and bridging bidentate coordination, and displaying molybdenum centers with tetrahedral, square-pyramidal, and octahedral coordination geometries.

The infrared spectrum of $[Mo_4O_{10}(OCH_3)_2(NNMePh)_2]^{2-}$ exhibits a strong band at 1594 cm^{-1} characteristic of ν(N=N) stretching mode of the coordinated hydrazido(2–) ligand, in addition to strong bands in the 925–770-cm^{-1} region attributable to Mo—O terminal and Mo—O—Mo bridging modes. Neither

Table II. Summary of Experimental Details for the X-ray Diffraction Studies of $(n\text{-}Bu_4N)_2[Mo_4O_{10}(OMe)_2(NNMePh)_2]$ (I) and $(n\text{-}Bu_4N)_2[Mo_4O_{12}(NHNC_8H_6N_4)]$ (II)

	I	II
(A) Crystal Parameters at 296 K[a]		
a, Å	9.770 (2)	16.528 (2)
b, Å	18.633 (3)	17.631 (3)
c, Å	16.706 (3)	19.539 (4)
α, deg	90.00	88.90 (1)
β, deg	90.74 (1)	87.00 (1)
γ, deg	90.00	88.10 (1)
V, Å^3	3041 (12)	5682.2 (24)
space group	$P2_1/c$	$P\bar{1}$
Z	2	4
ρ_{calcd}, g cm^{-3}	1.45	1.43
(B) Measurement of Intensity Data		
cryst shape and color	orange needles	reddish brown parallelepipeds
cryst dimens, mm	0.22 × 0.50 × 0.25	0.16 × 0.31 × 0.15
instrument	Nicolet R3m diffractomer	
radiation	Mo Kα (λ = 0.71073 Å)	
scan type	moving cryst—stationary counter	
scan range, deg	$2.0 < 2\theta \leq 45$	
scan length, deg	from $[2\theta(K\alpha_1) - 1.0]$ to $[2\theta(K\alpha_2) + 1.0]$	
ω–scan rate, deg/min	2–10	
ω–scan width, deg	1.2	1.2
bkgd meas	stationary cryst, stationary counter, at the beginning and end of each ω scan, each for half the time taken for the scan	
stds	3 collcd every 197 reflcns	
no. of reflcns collcd	2954 $(h,k,\pm l)$	11894 $(h,\pm k,\pm l)$
no. of reflcns used in solution ($F_o \geq 6\sigma(F_o)$)	1571	5429
(C) Reduction of Intensity Data and Summary of Structure Solution and Refinement[b]		
abs coeff, cm^{-1}	8.41	8.95
T_{max}/T_{min}	1.09	1.06
struct soln	Patterson synthesis yielded the Mo positions, all remaining non-hydrogen atoms located via standard Fourier techniques	
atom scattering factors[c]	neutral atomic scattering factors used throughout the analysis	
anomalous dispersion[d]	applied to all non-hydrogen atoms	
final discrepancy factors[e]		
R	0.0689	0.0647
R_w	0.0684	0.0686
goodness of fit[f]	1.32	1.57

[a] From a least-squares fitting of the setting angle of 25 reflections. [b] All calculations were performed on a Data General Nova 3 computer with 32K of 16-bit words using local versions of the Nicolet SHELXTL interactive crystallographic software package as described in: Sheldrick, G. M., *Nicolet SHELXTL Operations Manual*; Nicolet XRD Corp.: Cupertino, CA, 1979. Data were corrected for background, attenuators, and Lorentz and polarization effects in the usual fashion. [c] Cromer, D. T.; Mann, J. B. *Acta Crystallogr., Sect. A: Cryst. Phys., Diffr., Theor. Gen. Crystallogr.* **1968**, *24*, 321. [d] *International Tables for X-ray Crystallography*; Kynoch: Birmingham, England, 1962; Vol. III. [e] $R = \sum[|F_o| - |F_c|/\sum|F_o|]$; $R_w = [\sum w(|F_o| - |F_c|)^2/\sum w|F_o|^2]^{1/2}$; $w = 1/\delta^2(F_o) + g^*(F_o)$; $g = 0.002$. [f] GOF = $[\sum w(|F_o| - |F_c|)^2/(NO - NV)]^{1/2}$, where NO is the number of observations and NV is the number of variables.

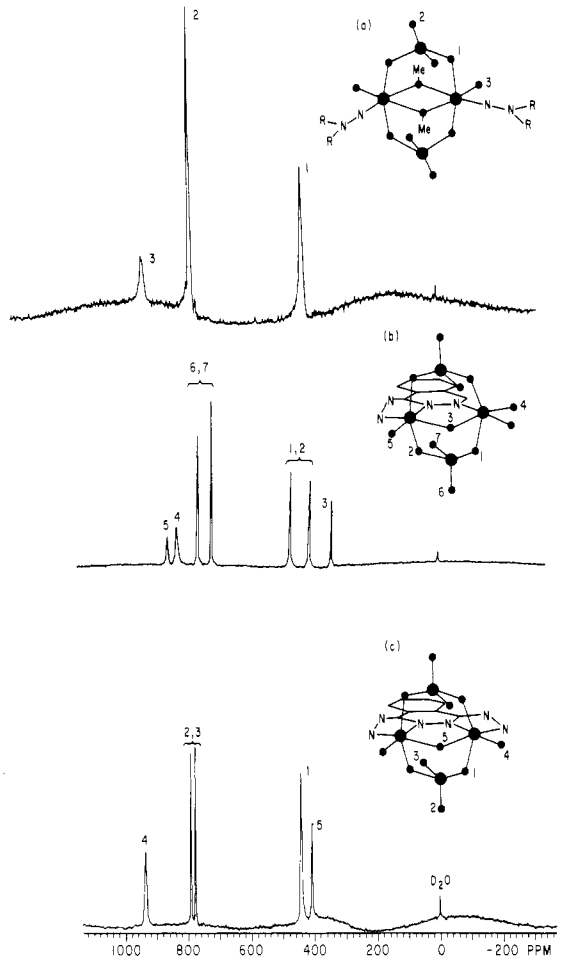

Figure 1. (a) Idealized bond structure of $[Mo_4O_{10}(OMe)_2(NNMePh)_2]^{2-}$, with one member from each set of equivalent oxygen atoms labeled, and the ^{17}O nmr spectrum of $[Mo_4O_{10}(OMe)_2(NNMePh)_2]^{2-}$. (b) Idealized bond structure of $[Mo_4O_{12}(C_8H_6N_4)]^{2-}$, with one member from each set of equivalent oxygen atoms labeled, and the ^{17}O NMR spectrum. (c) Idealized bond structure of $[Mo_4O_{11}(C_8H_6N_6)]^{2-}$, with one member from each set of equivalent oxygen atoms labeled, and the ^{17}O NMR spectrum.

the hydralazine derivative $[Mo_4O_{12}(C_8H_6N_4)]^{2-}$ nor the hydrazinophthalazine species $[Mo_4O_{11}(C_8H_6N_6)]^{2-}$ display bands characteristic of $\nu(N{=}N)$ stretching modes in the 1500–1650-cm^{-1} region. Absorptions assignable to the bent hydrazido(2-) unit are generally difficult to locate as these are considerably less intense than those associated with linear ($M{=}N{=}NR_2$) linkages and shifted to lower frequency as a consequence of less effective localization of multiple bond character in the N-N bond.

The electronic spectrum of $[Mo_4O_{10}(OCH_3)_2(NNMePh)_2]^{2-}$ is characterized by intense charge-transfer bands in the 250–350-nm region. In addition to absorbances in this region, the electronic spectra of $[Mo_4O_{12}(C_8H_6N_4)]^{2-}$ and $[Mo_4O_{11}(C_8H_6N_6)]^{2-}$ display a band in the 480–550-nm range with an extinction coefficient of ca. 5×10^3 M^{-1} cm^{-1}, which may be characteristic of the molybdenum–phthalazine bridging unit.

A fundamental spectroscopic description of oxomolybdate species is provided by the ^{17}O NMR spectrum, which yields information based on the general correlation between downfield chemical shift and oxygen π-bond order.[18,19] The ^{17}O NMR data for the complexes of this study are presented in Table I, and representative spectra are shown in Figure 1.

The ^{17}O spectra of the complex polyanions display the anticipated overall patterns. Bridging oxo groups appear in the 300–500 ppm range, while terminal oxo groups lie within the 750–950 ppm range characteristic of Mo(VI)–oxo compounds.[18] The linear correlation that exists between Mo–O π-bond order and ^{17}O chemical shift has been interpreted in terms of increasing π-bond order augmenting the paramagnetic screening of the oxygen nucleus, resulting in a larger chemical shift relative to $H_2{}^{17}O$. The rather broad widths at half-height for the ^{17}O signals are indicative of polynuclear species in solution.

A more detailed analysis of the ^{17}O spectra may be developed by comparing the spectra to those of other derivatized clusters. The tetranuclear species $[Mo_4O_8(OMe)_2(NNMePh)_2]^{2-}$ as shown by the schematic of Figure 1a and the structural discussion to follow, displays three nonequivalent sets of oxo groups, two terminal, O(2) and O(3), and one bridging, O(1). The bridging oxo groups are assigned unambiguously to the 425 ppm resonance. A range of 730–790 ppm appears to be characteristic for terminal oxo groups of a bidentate bridging $[MoO_4]^{2-}$ unit possessing terminal cis oxo groups, since $[Mo_8O_{26}]^{4-}$, $[Mo_4O_8(OCH_3)_2(NNAr)_4]^{2-}$, $[Mo_4O_{10}(OCH_3)_2(NNPh)_2]^{4-}$, and $Mo_8O_{20}(NNPh)_6]^{4-}$ all display resonances in this region assignable to this type of terminal oxo group.[20] The 932 and 781 ppm resonances may thus be assigned to O(3) and O(2), respectively. Although intensities of ^{17}O NMR resonances provide only a qualitative measure of the relative number of oxygen nuclei, the relative peak heights of the resonances at 932 and 781 ppm for $[Mo_4O_{10}(OMe)_2(NNMePh)_2]^{2-}$ also support the assignments of these resonances to O(3) and O(2), respectively. Alkoxy oxygen atoms are not observed as these do not exchange with ^{17}O oxo groups and hence are not enriched.[21]

The structure of the tetranuclear polyanion $[Mo_4O_{11}(C_8H_6N_6)]^{2-}$ is shown schematically in Figure 1c, illustrating the five nonequivalent oxo environments. Once again the 445 ppm resonance is assigned to the doubly bridging oxo groups O(1). The 408 ppm resonance is thus associated with the doubly bridging oxo group O(5). The resonances at 779 and 794 ppm are in the region characteristic for terminal oxo groups of the bidentate bridging $[MoO_4]^{2-}$ unit, O(2) and O(3). The structure of $[Mo_4O_{11}(C_8H_6N_6)]^{2-}$ reveals the structural and chemical inequivalence of O(2) and O(3), which gives rise to the two signals of approximately equal intensity. The 937 ppm resonance is the region characteristic of a single terminal oxo group, O(4), coordinated to a pseudooctahedral Mo(VI) site. The downfield position of O(4), relative to terminal cis oxo group resonances, is consistent with the greater degree of π interaction available to O4 in the absence of competition for the Mo t_{2g} type orbitals in the absence of other strong π-ligands.

Inspection of the schematic for the structure of $[Mo_4O_{12}(C_8H_6N_4)]^{2-}$, Figure 1b, reveals seven nonequivalent oxygen environments. By comparison with the assignments for bridging oxo groups associated with the $[MoO_4]^{2-}$ unit for $[Mo_4O_{10}(OCH_3)_2(NNMePh)_2]^{2-}$ and $[Mo_4O_{11}(C_8H_6N_6)]^{2-}$, the resonances at 404 and 463 ppm are assigned to O(1) and O(2). These two resonances may not be assigned unambiguously with the data available. The 355 ppm resonance is assigned with confidence to O(3). The relative chemical shifts, together with the relative intensities of the signals allows the assignment of the 792 and 835 ppm resonances to O(6) and O(7) of the bidentate $[MoO_4]^{2-}$ units, although again no unique assignment is posed. The low molecular symmetry of $[Mo_4O_{12}(C_8H_6N_4)]^{2-}$ results in the nonequivalence of the O(4) and O(5) sites. In fact, the two oxygen atoms of O(4) type are in nonequivalent chemical environments, which may result in broadening of the resonance associated with O(4), if not unique signals. The unusual broadness of the 897 ppm signal, together with the greater intensity relative to the 928 ppm signal, suggests that it be assigned to O4 environments. The assignment of the 928 ppm signal to O(5) is consistent with chemical shifts observed for single terminal oxo groups associated with $[MoO_2(\mu\text{-}O)_3N]$ and $[MoO(\mu\text{-}O)_3N_2]$ sites, which fall in the 930–940 ppm range.

In common with the type II or *cis*-dioxo isopoly oxomolybdate structures,[22] the electrochemistry of complexes I–III, as monitored

(18) Klemperer, W. G. *Angew. Chem., Int. Ed. Engl.* **1978**, *17*, 246.
(19) Kidd, R. G. *Can. J. Chem.* **1967**, 45, 605.
(20) Hsieh, T.-C.; Shaikh, S. N.; Zubieta, J. *Inorg. Chem.* **1987**, *26*, 4079.
(21) Chisholm, M. H.; Folting, K.; Hoffman, J. C.; Kirkpatrick, C. C. *Inorg. Chem.* **1984**, *23*, 1021.

Table III. Atom Coordinates ($\times 10^4$) and Temperature Factors (Å^2 $\times 10^3$) for $[Mo_4O_{10}(OCH_3)_2(MePhN_2)_2][n\text{-}Bu_4N]_2$

atom	x	y	z	U_{eq}[a]
Mo(1)	1178 (1)	5763 (1)	5175 (1)	48 (1)
Mo(2)	−718 (1)	4993 (1)	6631 (1)	37 (1)
O(1)	−764 (5)	5420 (3)	4650 (3)	58 (2)
O(2)	856 (5)	6669 (3)	4909 (3)	57 (2)
O(3)	154 (6)	5779 (3)	6232 (3)	63 (2)
O(4)	1867 (5)	5431 (3)	4105 (3)	55 (2)
O(5)	416 (5)	4417 (3)	7088 (3)	58 (2)
O(6)	−1755 (4)	5288 (2)	7346 (3)	42 (2)
N(1)	2790 (6)	5783 (3)	5594 (4)	50 (2)
N(2)	4086 (7)	5886 (4)	5824 (4)	63 (3)
N(3)	1409 (6)	7610 (3)	2652 (3)	38 (2)
C(1)	−1881 (9)	5937 (5)	4496 (5)	79 (4)
C(11)	4803 (7)	6554 (4)	5782 (4)	51 (3)
C(12)	6075 (8)	6661 (4)	6023 (5)	60 (3)
C(13)	6687 (9)	7326 (4)	5909 (5)	63 (3)
C(14)	5988 (8)	4870 (5)	5572 (5)	75 (4)
C(15)	4742 (8)	7764 (4)	5318 (4)	51 (3)
C(16)	4081 (8)	7126 (4)	5404 (4)	61 (3)
C(21)	4808 (8)	5273 (4)	6156 (5)	58 (3)
C(30)	151 (8)	7567 (5)	3173 (5)	65 (3)
C(31)	−1019 (8)	8061 (4)	3010 (5)	59 (3)
C(32)	−2130 (9)	4958 (5)	3555 (5)	67 (3)
C(33)	−3266 (12)	8414 (6)	3465 (7)	112 (5)
C(34)	2058 (9)	8349 (5)	2706 (5)	69 (3)
C(35)	2464 (8)	8641 (4)	3483 (5)	60 (3)
C(36)	3018 (8)	9404 (4)	3451 (5)	66 (3)
C(37)	3492 (7)	9704 (4)	4232 (4)	51 (3)
C(38)	2439 (8)	7096 (4)	2973 (5)	60 (3)
C(39)	3747 (8)	6991 (4)	2563 (5)	63 (3)
C(40)	4685 (8)	6449 (4)	2950 (5)	62 (3)
C(41)	5862 (9)	6313 (5)	2534 (6)	89 (4)
C(42)	1095 (8)	7485 (4)	1793 (4)	50 (3)
C(43)	498 (7)	6772 (4)	1588 (4)	46 (3)
C(44)	402 (8)	6641 (4)	726 (5)	60 (3)
C(45)	−193 (12)	5953 (6)	485 (7)	115 (5)

[a] Equivalent isotropic U defined as one-third of the trace of the orthogonalized U_{ij} tensor.

Table IV. Selected Bond Lengths (Å) and Angles (deg) for $(n\text{-}Bu_4N)_2[Mo_4O_{10}(OMe)_2(NNMePh)_2]$ (I)

Mo(1)–O(1)	2.18 (1)	Mo(1)–O(4)	2.02 (1)
Mo(2)–O(3)	1.82 (1)	Mo(2)–O(6)	1.67 (2)
Mo(1)–O(2)	1.77 (1)	Mo(1)–N(1)	1.71 (1)
Mo(2)–O(4a)	1.83 (1)	Mo(1)–O(1a)	2.25 (1)
Mo(1)–O(3)	2.04 (1)	N(1)–N(2)	1.34 (2)
Mo(2)–O(5)	1.71 (1)		
O(1)–Mo(1)–O(2)	91.6 (2)	O(2)–Mo(1)–O(4)	97.5 (5)
O(3)–Mo(1)–O(4)	161.0 (5)	Mo(1)–N(1)–N(2)	170.0 (13)
O(1)–Mo(1)–O(3)	85.3 (4)	O(2)–Mo(1)–N(1)	104.0 (6)
O(3)–Mo(1)–N(1)	96.0 (6)	Mo(1)–O(1)–Mo(1a)	113.0 (2)
O(1)–Mo(1)–O(4)	81.5 (4)	O(2)–Mo(1)–O(1a)	158.1 (5)
O(3)–Mo(1)–O(1a)	78.9 (4)	O(3)–Mo(2)–O(4a)	112.7 (5)
O(1)–Mo(1)–N(1)	163.8 (5)	O(4a)–Mo(2)–O(5)	114.6 (2)
O(4)–Mo(1)–N(1)	93.0 (6)	O(3)–Mo(2)–O(5)	111.1 (7)
O(1)–Mo(1)–O(1a)	66.6 (5)	O(4a)–Mo(2)–O(6)	104.5 (2)
O(4)–Mo(1)–O(1a)	83.3 (4)	O(3)–Mo(2)–O(6)	106.6 (2)
O(2)–Mo(1)–O(3)	96.6 (5)	O(5)–Mo(2)–O(6)	106.5 (2)
N(1)–Mo(1)–O(1a)	97.8 (5)		

by cyclic voltammetry, consists of totally irreversible and ill-defined multielectron reductions at large negative potentials ($E < -1.50$ V vs $Ag^+/AgCl$ reference). The absence of any oxidative processes suggests that the hydrazido-coordinated Mo centers behave as Mo(VI) centers with the nitrogenous ligand formally described as the hydrazido(2−) species. The behavior contrasts with that of mononuclear Mo–hydrazido complexes, which generally exhibit well-resolved oxidative and reductive processes in their electrochemistry.[23]

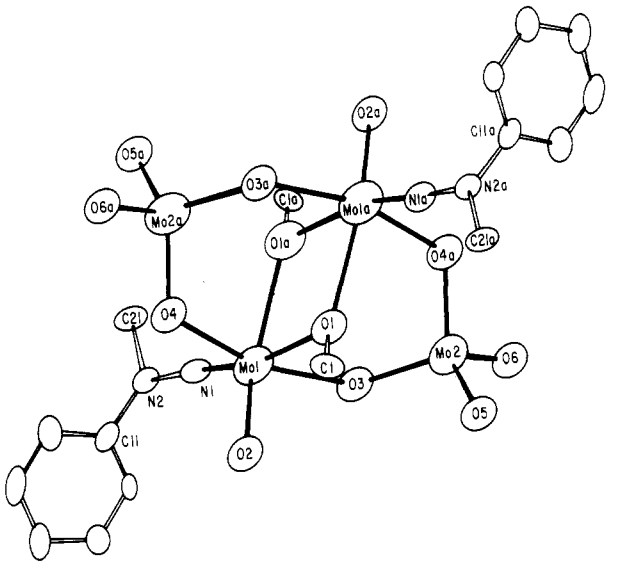

Figure 2. ORTEP view of the complex anion $[Mo_4O_{10}(OCH_3)_2(NNMePh)_2]^{2-}$, showing the atom-labeling scheme.

Description of the Structures. The structure of the $[Mo_4O_{10}(OCH_3)_2(NNMePh)_2]^{2-}$ complex anion is displayed in Figure 2; atomic positional parameters and selected bond lengths and angles are given in Tables III and IV, respectively. The anion crystallizes as discrete tetranuclear units incorporating coordinatively bound hydrazido(2−) groups. The overall geometry may be described in terms of two *cis*-$[MoO(NNR_2)]^{2+}$ units bridged by two methoxy groups and two $[MoO_4]^{2-}$ moieties, functioning as bidentate bridging ligands. The Mo(1)–O(1)–Mo(1a)–O(1a) rhombus is strictly planar as a consequence of the crystallographic center of symmetry located at the midpoint of the Mo(1a)–Mo(1a) vector.

The bridging $[MoO_4]^{2-}$ units display tetrahedral geometry about the molybdenum atoms, with unexceptional bonding parameters. The hydrazido-coordinated molybdenum centers enjoy distorted octahedral geometry $[MoO_5N]$ through ligation to the bridging oxygen donors of the methoxy groups, to the bridging oxo groups of the $[MoO_4]^{2-}$ units, to the terminal oxo groups and to the α-nitrogen of the terminal linear hydrazido(2−) ligand, with bond distances of 2.218 (5) Å (av), 2.029 (5) Å (av), 1.773 (5), and 1.715 (6) Å, respectively. The short Mo–N and N–N bond distances of 1.715 (6) and 1.332 (9) Å, respectively, together with the Mo–N–N bond angle of 170.0 (5)° indicate extensive delocalization throughout the $[Mo(N_2R_2)]$ unit and are consistent with the description of the organonitrogen ligand as the four-electron-donating organohydrazido(2−) species. Canonical forms A and B appear to be the major contributors to the overall electronic structures of the unit.

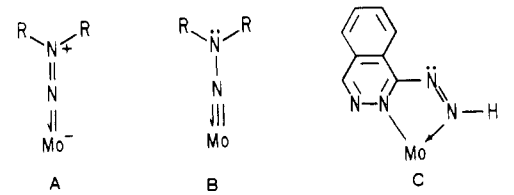

The structure of $[Mo_4O_{10}(OCH_3)_2(NNMePh)_2]^{2-}$ is similar to that of $[Mo_4O_8(OCH_3)_2(NNPh)_4]^{2-}$, with the exception that in the latter case, the nitrogen coordinated Mo centers display the *cis*-bis(diazenido)molybdenum core $[Mo(NNR)_2]^{2+}$, in contrast to the *cis*-oxo(hydrazido)molybdenum core of I.

Atomic positional parameters and structural parameters for the related tetranuclear derivatized oxomolybdate $[Mo_4O_{12}(C_8H_6N_4)]^{2-}$ are summarized in Tables V and VI respectively.

(22) Pope, M. T. *Inorg. Chem.* **1972**, *11*, 1973.
(23) Chrichton, B. A. L.; Dilworth, J. R.; Pickett, C. J. *J. Chem. Soc., Dalton Trans.* **1981**, 419.
(24) Dilworth, J. R.; Dahlstrom, P. L.; Hyde, J. R.; Kustyn, M.; Zubieta, J. *Inorg. Chem.* **1980**, *19*, 3562.
(25) Mattes, R.; Scholand, H. *Angew. Chem., Int. Ed. Engl.* **1983**, 22, 245.

Table V. Atom Coordinates ($\times 10^4$) and Temperature Factors ($Å^2 \times 10^3$) for $[Mo_4O_{11}(\mu\text{-}O)(HNN\text{-}pht)][n\text{-}Bu_4N]_2$ (II)

atom	x	y	z	U_{iso}	atom	x	y	z	U_{iso}
Mo(1)	1339 (1)	3862 (1)	8869 (1)	45 (1)[a]	C(25)	8643 (14)	4144 (12)	-288 (11)	59 (7)
Mo(2)	1252 (1)	4966 (1)	7465 (1)	40 (1)[a]	C(26)	8122 (15)	4208 (13)	-924 (12)	74 (8)
Mo(3)	1253 (2)	3716 (1)	6219 (1)	63 (1)[a]	C(27)	8565 (17)	4884 (15)	-1351 (13)	87 (9)
Mo(4)	2100 (1)	2921 (1)	7555 (1)	37 (1)[a]	C(28)	8074 (21)	5029 (18)	-2014 (17)	132 (12)
Mo(5)	6226 (1)	1139 (1)	3787 (1)	54 (1)[a]	C(29)	8547 (14)	2729 (12)	-245 (11)	58 (7)
Mo(6)	6915 (1)	2128 (1)	2424 (1)	42 (1)[a]	C(30)	8443 (16)	1976 (15)	232 (13)	86 (9)
Mo(7)	6141 (1)	1382 (1)	1109 (1)	57 (1)[a]	C(31)	8430 (18)	1340 (17)	-324 (15)	107 (10)
Mo(8)	6176 (1)	97 (1)	2361 (1)	43 (1)[a]	C(32)	8498 (26)	577 (23)	121 (20)	103 (14)
O(1)	1554 (10)	4030 (8)	9689 (6)	64 (6)[a]	C(33)	7481 (15)	3516 (13)	402 (11)	64 (7)
O(2)	381 (9)	3528 (8)	8912 (7)	59 (7)[a]	C(34)	7229 (15)	4302 (13)	675 (11)	63 (7)
O(3)	1361 (8)	4835 (6)	8461 (6)	46 (6)[a]	C(35)	6275 (19)	4292 (17)	846 (14)	108 (10)
O(4)	2116 (8)	3173 (6)	8568 (6)	43 (5)[a]	C(36)	5919 (18)	5099 (16)	1010 (14)	101 (10)
O(5)	233 (9)	5125 (7)	7473 (7)	55 (7)[a]	C(37)	7994 (15)	3327 (12)	4201 (11)	63 (7)
O(6)	1637 (9)	5861 (7)	7424 (7)	56 (6)[a]	C(38)	7297 (17)	3145 (14)	4706 (13)	82 (8)
O(7)	1330 (8)	3780 (6)	7544 (6)	37 (5)[a]	C(39)	6538 (19)	3553 (16)	4363 (15)	106 (10)
O(8)	1721 (9)	2051 (7)	7657 (7)	61 (6)[a]	C(40)	5732 (33)	3415 (28)	4802 (26)	116 (18)
O(9)	1973 (8)	2988 (7)	6535 (6)	46 (6)[a]	C(41)	8930 (14)	2248 (12)	4660 (11)	57 (7)
O(10)	1390 (9)	4699 (6)	6498 (6)	47 (6)[a]	C(42)	8750 (15)	1737 (14)	4056 (12)	74 (8)
O(11)	255 (10)	3437 (9)	6381 (10)	105 (9)[a]	C(43)	8929 (21)	876 (17)	4289 (15)	110 (11)
O(12)	1405 (13)	3738 (9)	5370 (8)	115 (10)[a]	C(44)	9799 (29)	758 (24)	4123 (22)	115 (15)
O(13)	6561 (8)	-814 (7)	2320 (7)	48 (6)[a]	C(45)	9442 (14)	3297 (12)	3899 (10)	54 (7)
O(14)	5174 (8)	-24 (8)	2418 (8)	62 (7)[a]	C(46)	10331 (16)	3038 (14)	4001 (12)	78 (8)
O(15)	6171 (8)	1291 (6)	2403 (7)	45 (6)[a]	C(47)	10873 (17)	3293 (14)	3333 (12)	83 (8)
O(16)	6355 (9)	219 (7)	3346 (7)	53 (6)[a]	C(48)	11801 (20)	3018 (17)	3413 (15)	117 (11)
O(17)	6536 (11)	968 (9)	4601 (7)	89 (8)[a]	C(49)	9007 (15)	3510 (13)	5136 (11)	72 (8)
O(18)	5227 (10)	1444 (9)	3851 (8)	82 (7)[a]	C(50)	8993 (15)	4402 (13)	5013 (12)	70 (8)
O(19)	6890 (10)	1883 (7)	3438 (6)	62 (6)[a]	C(51)	8886 (16)	4786 (13)	5732 (12)	78 (8)
O(20)	6473 (9)	3014 (7)	2504 (7)	64 (7)[a]	C(52)	8021 (20)	4715 (17)	6077 (15)	119 (11)
O(21)	6857 (9)	2094 (7)	1397 (7)	56 (6)[a]	C(53)	4195 (26)	2018 (21)	9048 (19)	115 (14)
O(22)	5140 (9)	1683 (9)	1211 (8)	81 (8)[a]	C(54)	4977 (35)	2169 (29)	9250 (27)	117 (18)
O(23)	6341 (11)	1355 (9)	257 (8)	92 (8)[a]	C(55)	5381 (30)	2477 (25)	8599 (23)	114 (16)
O(24)	6304 (9)	359 (7)	1391 (6)	49 (6)[a]	C(56)	6094 (33)	2860 (29)	8758 (25)	146 (19)
N(1)	3241 (10)	2484 (8)	7458 (7)	38 (5)	C(57)	3527 (27)	2331 (25)	10327 (21)	107 (15)
N(2)	3940 (11)	2853 (9)	7317 (8)	59 (5)	C(58)	3369 (30)	3048 (29)	10128 (24)	130 (17)
N(3)	3016 (9)	3839 (8)	7387 (7)	30 (4)	C(59)	3446 (33)	3629 (29)	10726 (26)	128 (18)
N(4)	2758 (10)	4599 (8)	7381 (7)	36 (5)	C(60)	3987 (35)	3790 (29)	11053 (27)	146 (20)
N(5)	8034 (10)	2528 (8)	2371 (7)	32 (4)	C(61)	3933 (26)	882 (23)	10101 (21)	171 (16)
N(6)	8716 (11)	2140 (9)	2288 (8)	47 (5)	C(62)	3490 (20)	639 (17)	10580 (16)	106 (11)
N(7)	7835 (11)	1184 (8)	2306 (7)	36 (4)	C(63)	3991 (18)	-13 (16)	10917 (14)	95 (9)
N(8)	7645 (10)	423 (8)	2300 (7)	39 (5)	C(64)	3506 (27)	-366 (24)	11489 (22)	111 (15)
N(9)	8373 (11)	3474 (9)	186 (8)	55 (5)	C(65)	2757 (24)	1511 (20)	9392 (19)	143 (13)
N(10)	8851 (10)	3097 (8)	4458 (7)	41 (5)	C(66)	2154 (23)	1617 (19)	9775 (17)	129 (12)
N(11)	3593 (15)	1798 (13)	9787 (11)	111 (8)	C(67)	1388 (20)	1321 (16)	9311 (15)	107 (10)
N(12)	3164 (15)	1543 (13)	5234 (12)	117 (8)	C(68)	588 (30)	1338 (25)	9720 (23)	121 (16)
C(1)	3328 (12)	5101 (11)	7269 (9)	42 (6)	C(69)	3043 (34)	2405 (29)	5133 (26)	146 (19)
C(2)	3740 (14)	3608 (11)	7291 (10)	47 (6)	C(70)	3731 (30)	2589 (26)	4761 (23)	129 (17)
C(3)	4147 (14)	4913 (11)	7177 (9)	36 (6)	C(71)	2617 (23)	3677 (21)	4825 (18)	133 (14)
C(4)	4742 (17)	5460 (15)	7060 (12)	81 (8)	C(72)	3642 (28)	4293 (25)	5399 (22)	149 (17)
C(5)	5555 (18)	5262 (15)	6945 (12)	88 (9)	C(73)	3888 (35)	1208 (24)	5281 (28)	63 (14)
C(6)	5794 (19)	4458 (15)	6943 (13)	94 (9)	C(74)	4131 (35)	1461 (36)	5901 (29)	95 (9)
C(7)	5238 (15)	3906 (15)	7069 (11)	75 (8)	C(75)	5114 (33)	1215 (29)	5911 (26)	82 (17)
C(8)	4421 (13)	4128 (11)	7168 (10)	50 (6)	C(76)	5500 (21)	1486 (18)	6478 (17)	133 (12)
C(11)	8232 (12)	-66 (11)	2233 (9)	42 (6)	C(77)	3640 (45)	885 (37)	4761 (39)	84 (17)
C(12)	8612 (14)	1387 (11)	2239 (9)	33 (5)	C(78)	2787 (46)	1184 (46)	4381 (37)	100 (14)
C(13)	9274 (15)	876 (11)	2202 (10)	51 (6)	C(79)	2849 (45)	219 (37)	3688 (34)	123 (24)
C(14)	10096 (16)	1064 (14)	2125 (11)	72 (8)	C(80)	2260 (44)	114 (36)	3465 (32)	116 (23)
C(15)	10712 (20)	491 (17)	2036 (14)	106 (10)	C(81)	2405 (19)	1210 (16)	5758 (15)	113 (11)
C(16)	10501 (19)	-278 (16)	2057 (13)	99 (10)	C(82)	1470 (37)	1400 (32)	5631 (30)	167 (22)
C(17)	9710 (16)	-479 (14)	2114 (11)	77 (8)	C(83)	1211 (18)	1210 (15)	6263 (14)	92 (9)
C(18)	9089 (15)	83 (12)	2154 (10)	49 (6)	C(84)	307 (23)	1466 (20)	6082 (18)	154 (14)
C(21)	8878 (13)	3455 (11)	846 (10)	48 (6)	C(85)	3119 (20)	1823 (18)	2286 (15)	127 (12)
C(22)	9778 (14)	3271 (12)	687 (11)	60 (7)	C(87)	4180 (30)	2088 (27)	2659 (24)	134 (18)
C(23)	10203 (16)	3310 (13)	1387 (12)	74 (8)	C(86)	9550 (26)	2802 (23)	7722 (20)	106 (15)
C(24)	11086 (17)	2994 (14)	1305 (12)	84 (9)					

[a] Equivalent isotropic U defined as one-third of the trace of the orthogonalized U_{ij} tensor.

As illustrated in Figure 3, the overall structure consists of a planar $[Mo_2O_4(HNN\text{-}pht)]^{2+}$ core bridged by two bidentate $[MoO_4]^{2-}$ units. The two tetranuclear dianions contained in the asymmetric unit display essentially identical structural features.

In common with the prototypical tetranuclear structure, $[Mo_4O_{10}(OCH_3)_2(NNR_2)_2]^{2-}$ and $[Mo_4O_8(OCH_3)_2(NNPh)_4]^{2-}$, the bidentate bridging $[MoO_4]^{2-}$ groups of $[Mo_4O_{12}(C_8H_6N_4)]^{2-}$ exhibit essentially identical coordination geometry, approximating the tetrahedral limit. The Mo centers of the planar binuclear oxobridged core $[Mo_2O_4(HNN\text{-}pht)]^{2+}$ display six-coordinate geometry, distorted from the octahedral limit. Although the gross structural relationship of $[Mo_4O_{12}(C_8H_6N_4)]^{2-}$ to the tetranuclear prototype $[Mo_4O_{10}(OCH_3)_2(NNR_2)_2]^{2-}$ is evident, there are a number of significant differences in the detailed coordination geometries of the nitrogen-ligated pseudooctahedral centers. In contrast to the identical Mo centers in the $[Mo_2O_2(OCH_3)_2(NNR_2)_2]^{2+}$ core of $[Mo_4O_{10}(OCH_3)_2(NNR_2)_2]^{2+}$, the $[Mo_2O_4(HNN\text{-}pht)]^{2+}$ moiety of II displays nonequivalent Mo

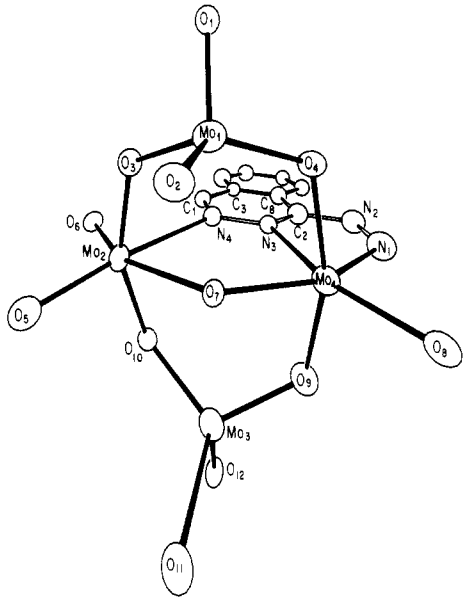

Figure 3. ORTEP view of the structure of $[Mo_4O_{12}(C_8H_6N_4)]^{2-}$, showing the atom-labeling scheme.

geometries. Hence, with molecule I used as representative of the substitution properties, Mo2 displays $[MoO_5N]$ coordination through ligation to the bridging oxo groups of the $[MoO_4]^{2-}$ units, to the bridging oxo group O(7) of the planar core, to two terminal oxo groups, and to a nitrogen donor of the bridging phthalazine ligand. In contrast, Mo4 exhibits $[MoO_4N2]$ coordination as a result of the substitution of the α-N donor of the hydrazido functionality for a terminal oxo group. The coordination geometry about Mo4 is thus defined by two bridging oxo groups from $[MoO_4]^{2-}$ units, the bridging oxo group O(7), a single terminal oxo group, and the nitrogen donors from the bridging phthalazine groups and from the hydrazido substituent of the hydralazine ligand.

Several features of the geometry of II merit discussion. The Mo–phthalazine N distances, Mo(2)–N(4) and Mo(4)–N(3), are significantly different, 2.55 (2) and 2.26 (1) Å, respectively. While the Mo(4)–N(3) distance is consistent with a Mo–N single bond, the Mo(2)–N(4) distance implies a bond order of less than 0.5. This observation cannot be accounted for simply on the basis of the trans influence of O(5), since N(3) is also disposed trans to a terminal oxo group. The nonequivalence of the Mo–N distances may be related to the requirements of chelate ring formation shortening the Mo(4)–N(3) distance and to the electronic and steric requirements of the dioxo unit of Mo(2) forcing the lengthening of an in-plane Mo–N interaction. If it is assumed that the total bond orders about Mo(2) and Mo(4) are nearly equal, the Mo(2)–N(4) interaction coplanar with a cis $Mo–O_2$-(terminal) unit should be significantly weaker than that of the Mo(4)–N(3) bond attached to a molybdenum center with a single terminal oxo group. Similar effects have been observed in other polyoxoanion structures.[26,27] The long Mo–N bond distances indicate weak interactions, reflecting the absence of a strong electrostatic component to the bonding, a common observation for interactions between Mo(VI) and neutral base ligands.[6]

The bond distances from the six-coordinate Mo centers to the bridging oxo groups of the $[MoO_4]^{2-}$ units are also nonequivalent, with Mo(2)–O_b of 1.96 (1) Å and Mo(4)–O_b of 2.02 (1) Å. A similar pattern of bond lengths is observed for $[Mo_4O_{10}(OCH_3)_2(NNPh)_2]^{2-}$.[20] Although it is generally anticipated that the shorter bond distances will be associated with the O_b–Mo–O_b valence angle most closely approaching the 180° idealized limit in order to maximize overlap with the Mo bonding orbitals, it is noteworthy that in both instances the shorter bond lengths are associated with the bond angle displaying the larger deviation from 180°. These observations suggest a cis influence of the *cis*-dioxo unit, $[MoO_2]^{2+}$, resulting in an overall decrease in the bond distance relative to the *cis*-oxohydrazido $[MoO(NHNR)]^{2+}$ or

Table VI. Selected Bond Lengths (Å) and Angles (deg) for $(n\text{-}Bu_4N)_2[Mo_4O_{12}(HNN\text{-}pht)]$ (II)

molecule 1		molecule 2	
Mo(1)–O(1)	1.69 (3)	Mo(5)–O(16)	1.85 (1)
Mo(1)–O(2)	1.71 (1)	Mo(5)–O(17)	1.71 (2)
Mo(1)–O(3)	1.88 (1)	Mo(5)–O(18)	1.72 (1)
Mo(1)–O(4)	1.82 (1)	Mo(5)–O(19)	1.84 (1)
Mo(2)–O(3)	1.97 (1)	Mo(8)–O(13)	1.71 (1)
Mo(2)–O(5)	1.70 (1)	Mo(8)–O(14)	1.68 (1)
Mo(2)–O(6)	1.72 (1)	Mo(8)–O(15)	2.11 (1)
Mo(2)–O(7)	2.09 (1)	Mo(8)–O(16)	1.98 (1)
Mo(2)–O(10)	1.96 (1)	Mo(8)–O(24)	1.95 (1)
Mo(2)–N(4)	2.55 (2)	Mo(8)–N(8)	2.52 (2)
Mo(3)–O(9)	1.84 (1)	Mo(7)–O(21)	1.87 (1)
Mo(3)–O(10)	1.85 (1)	Mo(7)–O(22)	1.72 (2)
Mo(3)–O(11)	1.75 (2)	Mo(7)–O(23)	1.68 (2)
Mo(3)–O(12)	1.67 (2)	Mo(7)–O(24)	1.89 (1)
Mo(4)–O(4)	2.04 (1)	Mo(6)–O(15)	1.96 (1)
Mo(4)–O(7)	1.95 (1)	Mo(6)–O(19)	2.02 (1)
Mo(4)–O(8)	1.68 (1)	Mo(6)–O(20)	1.71 (1)
Mo(4)–O(9)	2.02 (1)	Mo(6)–O(21)	2.02 (1)
Mo(4)–N(1)	2.01 (2)	Mo(6)–N(5)	2.00 (2)
Mo(4)–N(3)	2.26 (2)	Mo(6)–N(7)	2.23 (2)
O(1)–Mo(1)–O(2)	105.5 (7)	O(16)–Mo(5)–O(17)	105.6 (7)
O(1)–Mo(1)–O(3)	102.7 (6)	O(16)–Mo(5)–O(18)	111.7 (7)
O(1)–Mo(1)–O(4)	104.9 (6)	O(16)–Mo(5)–O(19)	114.5 (6)
O(2)–Mo(1)–O(3)	111.0 (6)	O(17)–Mo(5)–O(18)	107.7 (8)
O(2)–Mo(1)–O(4)	114.1 (6)	O(17)–Mo(5)–O(19)	104.6 (7)
O(3)–Mo(2)–O(4)	117.1 (5)	O(18)–Mo(5)–O(19)	112.0 (7)
O(3)–Mo(2)–O(5)	98.3 (6)	O(13)–Mo(8)–O(14)	102.7 (7)
O(3)–Mo(2)–O(6)	94.7 (6)	O(13)–Mo(8)–O(15)	158.4 (6)
O(3)–Mo(1)–O(7)	79.9 (5)	O(13)–Mo(8)–O(16)	95.4 (6)
O(3)–Mo(2)–O(10)	156.5 (5)	O(13)–Mo(8)–O(24)	97.9 (6)
O(3)–Mo(2)–N(4)	84.6 (5)	O(13)–Mo(8)–N(8)	83.3 (6)
O(5)–Mo(2)–O(6)	104.0 (6)	O(14)–Mo(8)–O(15)	98.9 (6)
O(5)–Mo(2)–O(7)	101.3 (6)	O(14)–Mo(8)–O(16)	98.8 (7)
O(15)–Mo(2)–O(10)	96.2 (6)	O(14)–Mo(8)–O(24)	99.1 (7)
O(5)–Mo(2)–N(4)	173.8 (6)	O(14)–Mo(8)–N(8)	174.0 (6)
O(6)–Mo(2)–O(7)	154.7 (6)	O(15)–Mo(8)–O(16)	80.3 (5)
O(6)–Mo(2)–O(10)	99.6 (6)	O(15)–Mo(8)–O(24)	79.4 (5)
O(6)–Mo(2)–N(4)	81.2 (6)	O(15)–Mo(8)–N(8)	75.2 (5)
O(7)–Mo(2)–O(10)	79.2 (5)	O(16)–Mo(8)–O(24)	154.7 (6)
O(9)–Mo(3)–O(10)	116.3 (6)	O(21)–Mo(7)–O(22)	112.9 (7)
O(9)–Mo(3)–O(11)	110.6 (7)	O(21)–Mo(7)–O(23)	103.4 (7)
O(9)–Mo(3)–O(12)	105.8 (7)	O(21)–Mo(7)–O(24)	118.1 (6)
O(10)–Mo(3)–O(11)	111.5 (7)	O(22)–Mo(7)–O(23)	105.3 (8)
O(10)–Mo(3)–O(12)	105.7 (7)	O(22)–Mo(7)–O(24)	112.3 (7)
O(11)–Mo(3)–O(12)	106.1 (10)	O(23)–Mo(7)–O(24)	103.0 (7)
O(4)–Mo(4)–O(7)	82.6 (5)	O(15)–Mo(6)–O(19)	83.5 (6)
O(4)–Mo(4)–O(8)	97.3 (6)	O(15)–Mo(6)–O(20)	115.9 (6)
O(4)–Mo(4)–O(9)	163.4 (5)	O(15)–Mo(6)–O(21)	83.0 (6)
O(4)–Mo(4)–N(1)	96.8 (6)	O(15)–Mo(6)–N(5)	151.3 (5)
O(4)–Mo(4)–N(3)	85.7 (5)	O(15)–Mo(6)–N(7)	81.9 (6)
O(7)–Mo(4)–O(8)	117.3 (6)	O(19)–Mo(6)–O(20)	95.7 (6)
O(7)–Mo(4)–O(9)	82.0 (5)	O(19)–Mo(6)–O(21)	165.3 (5)
O(7)–Mo(4)–N(1)	151.1 (6)	O(19)–Mo(6)–N(5)	95.6 (6)
O(7)–Mo(4)–N(3)	82.9 (5)	O(19)–Mo(6)–N(7)	86.5 (5)
O(8)–Mo(4)–O(9)	95.3 (6)	O(20)–Mo(6)–O(21)	95.6 (6)
O(8)–Mo(4)–N(1)	91.5 (7)	O(20)–Mo(6)–N(5)	92.8 (7)
O(8)–Mo(4)–N(3)	159.8 (6)	O(20)–Mo(6)–N(7)	162.2 (7)
O(9)–Mo(4)–N(1)	93.6 (6)	O(21)–Mo(6)–N(5)	93.4 (6)
O(9)–Mo(4)–N(3)	89.1 (5)	O(21)–Mo(6)–N(7)	85.8 (5)
N(1)–Mo(4)–N(3)	68.3 (6)	N(5)–Mo(6)–N(7)	69.4 (6)
Mo(4)–N(1)–N(2)	128.5 (12)	Mo(6)–N(5)–N(6)	127.4 (12)
Mo(2)–N(4)–N(3)	120.7 (11)	Mo(6)–N(7)–N(8)	123.8 (13)
Mo(4)–N(3)–N(4)	119.9 (11)	Mo(8)–N(8)–N(7)	118.1 (11)
Mo(2)–O(7)–Mo(4)	142.7 (7)	Mo(6)–O(15)–Mo(8)	140.8 (7)

(26) Schroder, F. A. *Acta Crystallogr., Sect. B: Struct. Crystallogr. Cryst. Chem.* **1975**, *B31*, 2294.
(27) Bart, J. C. J.; Ragaini, V. In *Proceedings of the Climax 3rd International Conference on the Chemistry and Uses of Molybdenum*; Baruy, M. F., Mitchell, P. C. H., Eds.; Climax Molybdenum Co.: Ann Arbor, MI, 1979.

Table VII. Comparison of Structural Parameters for the Structures of $(n\text{-}Bu_4N)_2[Mo_4O_{10}(OMe)_2(NNMePh)_2]$ (I), $(n\text{-}Bu_4N)_2[Mo_4O_{12}(HNN\text{-}pht)]$ (II) and $(Et_3NH)_2[Mo_4O_{11}(dhphH_2)]$ (III)[a,b]

		II		
	I	molecule 1	molecule 2	III
Mo_{tet}–O_t	1.67 (1)–1.71 (2)	1.67 (1)–1.75 (2)	1.68 (2)–1.72 (1)	1.691 (8)–1.731 (8)
Mo_{tet}–O_b	1.83 (1)	1.82 (1)–1.88 (1)	1.84 (1)–1.89 (1)	1.807 (6)–1.863 (6)
O–Mo_{tet}–O	104.5 (6)–114.6 (6)	102.7 (6)–117.1 (5)	104.6 (7)–118.1 (6)	102.8 (3)–1158 (3)
Mo_{oct}–O_t	1.77 (1)	1.68 (1)–1.72 (1)	1.68 (1)–1.71 (1)	1.697 (6)
Mo_{oct}–O_b	2.02 (1), 2.04 (1)	1.96 (1), 1.97 (1) [MoO_5N]	1.98 (1), 1.95 (1) [MoO_5N]	2.054 (6), 2.041 (6)
		2.04 (1), 2.02 (1) [MoO_4N_2]	2.02 (1), 2.02 (1) [MoO_4N_2]	
Mo_{oct}–O_b'	2.25 (1) (*O*-methoxy)	2.09 (1) [MoO_5N]	2.11 (1) [MoO_5N]	1.972 (6)
		1.95 (1) [MoO_4N_2]	1.96 (1) [MoO_4N_2]	
Mo_{oct}–N(pht)		2.55 (2) [MoO_5N_2]	1.96 (1) [MoO_4N_2]	2.187 (6)
		2.26 (2) [MoO_4N_2]	2.23 (2) [MoO_4N_2]	1.996 (7)
Mo_{oct}–N(hyd)	1.71 (2)	2.01 (2)	2.00 (2)	
O_b'-Mo_{oct}–N(pht)		73.7 (5) [MoO_5N]	75.2 (5) [MoO_5N]	81.8 (2)
		82.9 (5) [MoO_4N_2]	81.9 (6) [MoO_4N_2]	
O_t–Mo_{oct}–N(pht)		173.8 (6) [MoO_5N]	174.0 (6) [MoO_5N]	68.5 (3)
		159.8 (6) [MoO_4N_2]	162.2 (7) [MoO_4N_2]	
N(hyd)–Mo_{oct}–N(pht)		68.3 (6)	69.4 (6)	
Mo–N–N(hyd)	170.0 (13)	128.5 (12)	127.4 (12)	
N–N(hyd)	1.34 (2)	1.36 (2)	1.30 (2)	1.33 (1)
Mo–N–N(phth)		119.9 (11), 120.7 (11)	123.8 (12), 118.1 (11)	
N–N(phth)		1.39 (2)	1.39 (2)	1.369 (9)
Mo_{oct}–O_b'–Mo_{oct}	113.0 (2)	142.7 (7)	140.8 (7)	134.6 (3)
Mo–Mo	3.70	3.83	3.83	3.47

[a] Bond lengths in angstroms, bond angles in degrees. [b] Abbreviations: Mo_{tet}, pseudotetrahedral Mo centers; Mo_{oct}, pseudooctahedral Mo center; O_t, terminal oxo group; O_b, bridging oxo group from the $[MoO_4]^{2-}$ center; O_b', bridging oxo group between the Mo_{oct} centers; N(pht), phthalazine N donor; N(hyd), hydrazido N donor.

cis-diazenido $[Mo(NNR)_2]^{2+}$ groupings.

The metrical parameters for the five-membered chelate ring Mo–N(1)–N(2)–C(2)–N(3) and the planarity of the phthalazine group indicate extensive charge delocalization throughout the $(HNN\text{-}pht)^{2-}$ ligand. Comparison with similar structures[13,24,25] suggests that the ligand is best formulated as a doubly deprotonated hydrazido(2-) species, described by canonical form C, although direct crystallographic confirmation of the location of the nitrogen bound hydrogen was not possible. In this sense, the Mo4 center is described formally as a hydrazido(2-)–Mo(VI) species, in common with the formalism adopted for the related complex $[Mo_4O_{10}(OCH_3)_2(NNMePh)_2]^{2-}$. The structure of II is most clearly related to that previously described for the dihydrazido–phthalazine complex, $[Mo_4O_{11}(C_8H_6N_6)]^{2-}$, as illustrated in Table VII. The only significant structural differences between II and $[Mo_4O_{11}(C_8H_6N_6)]^{2-}$, shown schematically in Figure 1c, result from the substitution of a terminal oxo group of the planar core by a N donor of the additional hydrazido arm of the 1,4-dihydrazinophthalazine ligand. The major consequence is the geometric equivalence of the two Mo centers of the planar core $[Mo_2O_3(C_8H_6N_6)]^{2+}$, which display $[MoO_4N_2]$ pseudooctahedral coordination.

A Comment on the Oxidation States of the Molybdenum Centers. The tetranuclear complex $[Mo_4O_{11}(C_8H_6N_6)]^{2-}$ has been described as a mixed-valence complex of Mo(VI) and Mo(IV), using the neutral diazene formalism for the quadruply deprotonated (HN-N–C_8H_4–NNH) ligand.[13] We prefer the hydrazido(2-) formalism for the ligand and hence describe complexes I, II, and $[Mo_4O_{11}(C_8H_6N_6)]^{2-}$ as Mo(VI) species. The electronic spectra of the complexes are suggestive of a superposition of the spectra of $[Mo^{VI}O_4]$ centers and Mo–Oxohydrazido centers, that is, a strong charge-transfer band at ca. 200-250 nm, associated with the former, and a weaker transition at 480–530 nm, assigned to the presence of the *cis*-oxo(hydrazido)molybdenum(VI) unit. The absence of intervalence charge-transfer bands in the optical spectrum cannot be interpreted as evidence for the absence of mixed-valence states since the grossly different site symmetries of the Mo centers would result in a class I compound[28] that would not exhibit IVCT bands. However, the Mo(VI) assignment is supported by the absence of unusual chemical shifts in the ^{17}O NMR spectra and by electrochemical characteristics of these complexes. Well-behaved oxidation processes are characteristic of the cyclic voltammetry of Mo(IV)–hydrazino-type complexes. In contrast, type II poly oxomolybdate anions and derivatives are characterized by ill-behaved multielectron reductions and an absence of oxidative processes. The cyclic voltammograms of I, II, and $[Mo_4O_{11}(C_8H_6N_6)]^{2-}$, vide infra, show an absence of any oxidative processes and only ill-behaved reductions at potentials more negative than −1.5 V. We are currently undertaking a study of the ^{95}Mo NMR spectroscopy of these and related complexes in an effort to define unambiguously the oxidation states of the derivatized Mo centers.

Acknowledgment. This research was supported by NSF Grant CHE8514634.

Registry No. I, 105473-73-2; II, 114156-04-6; III, 114183-74-3.

Supplementary Material Available: Tables S.1–S.4 and S.6–S.9, listing bond distances, bond angles, anisotropic temperature factors, and calculated hydrogen atomic positions for structures I and II, respectively (16 pages); Tables S.5 and S.10, listing calculated and observed structure factors for I and II, respectively (103 pages). Ordering information is given on any current masthead page.

(28) Robin, M. B.; Day, P. *Adv. Inorg. Chem. Radiochem.* **1967**, 10, 247.